~~Strong response of the field-like spin-orbit torque to piezoelectric strain in perpendicularly magnetized $Ta/Co_{20}Fe_{60}B_{20}/Ta/MgO$ film~~ Joint effect of piezoelectric strain and current-induced heating on the field-like spin-orbit torque in perpendicularly magnetized $Ta/Co_{20}Fe_{60}B_{20}/Ta/MgO$ film

M. Filianina,[1,2] Z. Wang,[1,3] L. Baldrati,[1] K. Lee,[1] M. Vafaee,[1,4] G. Jakob,[1] and M. Kläui[1,2,a)]
[1)] *Institute of Physics, Johannes Gutenberg University, 55128 Mainz, Germany*
[2)] *Graduate School of Excellence Material Science in Mainz, 55128 Mainz, Germany*
[3)] *Department of Physics, Chang'an University, 710064 Xi'an, China*
[4)] *Singulus Technology AG, 63796 Kahl am Main, Germany*

(Dated: 8 December 2020)

Spin-orbit torques (SOTs) are known to be the most efficient way to manipulate the magnetization direction by electrical currents. While, conventionally, one symmetry component of the SOTs, namely the damping-like torque, was considered to play a primary role, recently the significance of the other component, the field-like torque, has been revised, owing to the non-trivial dynamics it can induce in heavy metal/ferromagnet multilayers. In this work, we first discuss the unusual behavior of the field-like SOT in a Ta/CoFeB/Ta/MgO multilayer system with a reduced magnetic anisotropy and demonstrate an energy-efficient approach to manipulate the magnitude of the SOT effective fields. Finally, our results show a possibility to engineer the anisotropy of the field-like SOTs by piezoelectric strain, which can be potentially attractive for application in spintronics.

Magnetic memories rely on using the magnetization direction to store information, thus, the optimization of the magnetization switching mechanisms has attracted significant research interest in recent years. Spin-orbit torques (SOT)s[1–6] are known to be the most energy-efficient approach to switch the magnetization direction by electrical currents, in both in-plane and out-of-plane magnetized ferromagnetic (FM) devices. As an example, the SOTs can arise in heavy-metal (HM)/FM structures (see Fig. 1 (a)), when an in-plane charge current is applied to the HM layer to generate an out-of-plane spin-polarized current due to the strong spin-orbit coupling (SOC). The spin torque from the spin-polarized current is transferred to the FM layer and influences the magnetization, which can be decomposed into a damping-like (DL) and a field-like (FL) contributions with different symmetries.[4,6] The magnitude of the SOTs limits the energy-efficiency of this approach. In turn, the magnitude of the SOTs can be optimized by judicious material engineering, tuning e.g. the composition of the layers or their thicknesses,[6] which imposes certain constraints as these parameters remain fixed once a device is fabricated. A dynamical tool to control the magnitudes of the SOTs that was recently found[7,8] is the use of mechanical strain.

Particularly attractive for the control of systems parameters, e.g. magnetic anisotropy,[9–12] is mechanical strain generated by piezoelectric effects.[13] That is because piezoelectric strain can be locally and reliably generated by energy-efficient electric fields utilizing commercially available piezoelectric substrates.[14] The analysis of the impact of strain on the magnetization switching by spin torques was addressed computationally.[7,15,16] It reveals that strain, affecting primarily the magnetic anisotropy, may lead to an improvement of the performances of SOT switching devices. Moreover, even in a system with perpendicular magnetic anisotropy (PMA), such as W/CoFeB/MgO,[8] where the strain-induced magnetic anisotropy is negligible compared to the interfacial anisotropy, the SOTs could be very sensitive to the strain state. In this case, the impact of strain was found to occur via changing the orbital polarization of the electronic states in the FM, dominating the hybridization with the electronic states in the HM underlayer, resulting in a strong tuning of the SOTs. Thus, it is interesting to explore further possibilities to tailor the SOTs by strain, for example, by considering a PMA system with a lower magnetic anisotropy, where the enhanced impact of strain on the magnetic anisotropy can possibly be expected.

In this work we experimentally investigate the SOTs in a perpendicularly magnetized multilayer $Ta(5)/Co_{20}Fe_{60}B_{20}(1)/Ta(0.08)/MgO(2)/Ta(3)$ stack deposited on a piezoelectric substrate. An additional ultrathin Ta interlayer is introduced to decrease the perpendicular magnetic anisotropy in the system,[17,18] thus, enabling an enhanced impact of electrically controlled strain on the magnetic properties. The SOTs are ascertained by magneto-transport and second-harmonic methods under in-plane strain of different direction and magnitude. Similarly to the conventional Ta-based CoFeB stacks, our system is characterized by a significantly larger magnitude of the FL SOT compared to the DL torque and we find that the magnitude of the FL SOT can be varied by modulating the piezoelectric strain with an electric field applied across the PMN-PT substrate. We explain this behavior of the FL SOTs by a combined action of the current-induced reduction of the magnetic anisotropy assisted or counteracted by the generated strain of different symmetry.

Figure 1 (a) shows the schematic of the device structure used in the experiment. The symmetric 1 μm-wide Hall cross devices were fabricated from a continuous single layer stack of $Ta(5)/Co_{20}Fe_{60}B_{20}(1)/Ta(0.08)/MgO(2)/Ta(3)$

[a)] Electronic mail: klaeui@uni-mainz.de.

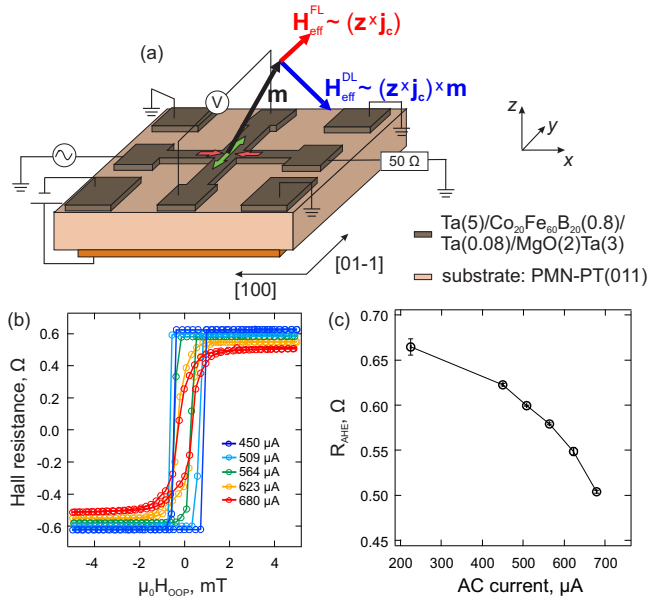

FIG. 1. (a) Schematic of the sample geometry showing the PMN-PT substrate with the Hall cross device used for the SOT measurements and the corresponding electrical connections. A positive electric field is applied in the OOP direction across the PMN-PT substrate to generate strain. Current-induced SOT effective fields are indicated. (b) Anomalous Hall resistance during the OOP magnetic field sweep acquired for various currents at room temperature and zero applied electric field across the PMN-PT substrate, showing the change of the loop shape with increasing current. (c) Current dependence of the R_{AHE} determined from the out-of-plane hysteresis loops shown in (b).

(thickness in parentheses is given in nm) as described in Supplementary Materials. For the electric field generation of strain a $[Pb(Mg_{0.33}Nb_{0.66}O_3)]_{0.68}$-$[PbTiO_3]_{0.32}(011)$ (PMN-PT) (011) substrate was used.[19]

First, we discuss the magnetic properties of the Ta/CoFeB/Ta/MgO system. The AHE resistance measured as a function of the perpendicular magnetic field under various input AC currents flowing along the [100] direction of the PMN-PT substrate is shown in Fig. 1 (b). In addition to the AHE resistance decrease, one can also observe that the shape of the hysteresis loops changes depending on the values of used current amplitudes. At lower currents, the loops have a square shape and abrupt switching at approximately 0.65 mT. For higher currents, the loops become more round and the coercive field is reduced (see Supplementary Materials).

Since the AHE in ferromagnets is proportional to the perpendicular component of the magnetization, M_z, the gradual decrease of the AHE resistance with increasing current, observed in Fig. 1 (b,c), can be related to a reduction of the magnetization.[20] This is consistent with the temperature behavior of the AHE resistance measured at low input AC currents (see Supplementary Materials). Similarly, in the literature, the temperature dependence of the AHE was explained by the temperature dependence of the magnetization.[21,22] Furthermore, both the change in the loops shape and the decreasing coercivity indicate a significant decrease of the PMA at higher currents. Thus, it can be assumed that, in our system, high currents with the associated Joule heating lead to a significant change of the magnetic properties, i.e. the reduction of M_s and the PMA.[3]

Next, we experimentally study the current-induced SOT effective fields in our system. To evaluate the SOT effective fields, we used the harmonic Hall voltage measurement technique[23,24] as described in Supplementary Materials. Figures 2 (a) and (b) present the first and the second harmonic signals measured as a function of the longitudinal (along the current direction) and transverse (perpendicular to the current direction) external magnetic fields, respectively, for zero electric field applied across the substrate. The AC current with the density of $(7.903 \pm 0.004) \times 10^{10}$ A m^{-2} is flowing along the compressive, [100], strain direction of the PMN-PT substrate. One can see that as compared to the slope of 2ω signal for the transverse field sweep, determining the FL SOT (Fig. 2 (b)), the slopes of the $V_{\mathrm{Hall}}^{2\omega}$ in Fig. 2 (a) are small even at a relatively high current density. These small $V_{\mathrm{Hall}}^{2\omega}$ signal slopes for the longitudinal field sweep hinder the robust estimation of the DL SOT for this system and the magnitude of the DL SOT is found to be smaller than (0.9 ± 0.5) mT$/10^{11}$ A m^{-2} at all magnitudes of the electric field applied across the PMN-PT substrate.

For the DL SOT is small and cannot be reliably determined in our system, we discuss next the properties of the FL SOTs. The current density dependence of the FL SOT effective fields are plotted in Fig. 2 (c) for different electric fields applied across the PMN-PT substrate. Firstly, we note that the SOT effective fields shown in red for zero electric field do not exhibit the typical behavior with a linear dependence on the current density, j_c, and zero values at $j_c = 0$.[3,25–27] On the contrary, the red solid line in Fig. 2 (c) represents the best fit to the data using a power law function converging with the power of 3.7. This suggests a significant contribution from non-linear effects such as the Joule heating effect,[28] which is in agreement with the AHE resistance behavior as a function of the AC current, seen in Figs. 1 (b,c).

Furthermore, it can be seen that the behavior gradually changes from the power law (red data set) to a more linear dependence (black data set) when the electric field across the PMN-PT substrate is increased. Figure 2 (d) shows the harmonic Hall signals as a function of the transverse magnetic field measured using similar current density and the same geometry as in (a) for the case of 300 kV m^{-1} applied across the PMN-PT substrate. One can immediately notice a significant change of the $V_{\mathrm{Hall}}^{2\omega}$ slope as compared to the case of zero applied electric field shown in Fig. 2 (b). Thus, one can directly see the difference in the FL SOT effective fields at zero and 300 kV m^{-1} and this difference becomes more pronounced at higher current densities. Remarkably, compared to the strain response of the SOTs in W/CoFeB/MgO multilayers,[8] the FL torque in this Ta/CoFeB/Ta/MgO system is much more sensitive to the piezoelectric strain.

We repeat the measurements of the FL SOT in the orthogonal configuration, i.e. when the AC current flows along the $[01\bar{1}]$ direction of the PMN-PT substrate. Thus, according

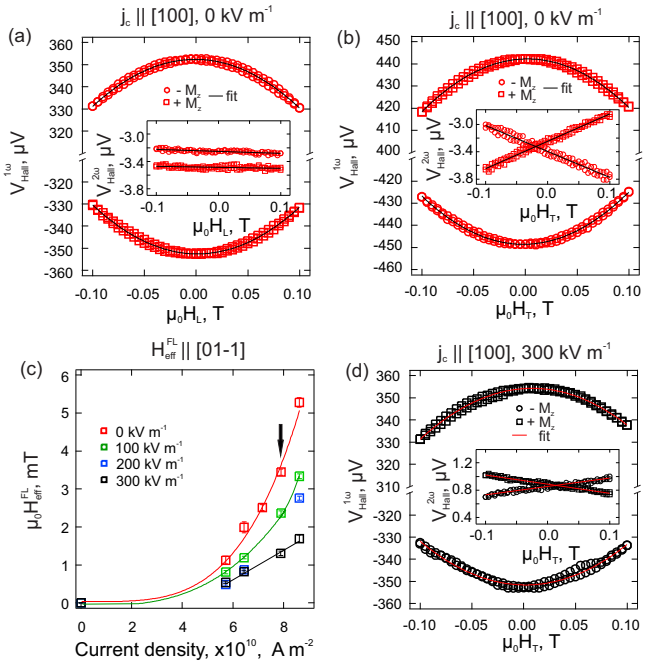

FIG. 2. First harmonic, $V_{\mathrm{Hall}}^{2\omega}$, and the second harmonic, $V_{\mathrm{Hall}}^{2\omega}$, Hall signals as a function of (a) the longitudinal and (b) transverse in-plane magnetic field at zero applied electric field across the PMN-PT substrate, measured using an AC current density of $(7.903 \pm 0.004) \times 10^{10}$ A m^{-2}. Circular and square-shaped symbols represent signals for the magnetization pointing along $-z$ and $+z$, respectively. The solid lines represent the linear and quadratic fitting curves. (c) The field-like SOT effective field plotted as a function of the current density when the current is flowing along the compressive ([100]) strain direction of the PMN-PT substrate (i. e. the FL SOT is along the tensile strain direction) measured at different electric fields applied across the substrate. Note that the data points represent the average values of the two values measured for opposite magnetization directions. The solid lines represent a power law fit to the data. (d) First harmonic, $V_{\mathrm{Hall}}^{1\omega}$, and the second harmonic, $V_{\mathrm{Hall}}^{2\omega}$, Hall signals as a function of the transverse magnetic field at 300 kV m^{-1} applied across the PMN-PT substrate, measured using the AC current density of $(7.886 \pm 0.004) \times 10^{10}$ A m^{-2}. The black arrow in (c) indicates the current density value at which the data in (a), (b) and (d) were acquired.

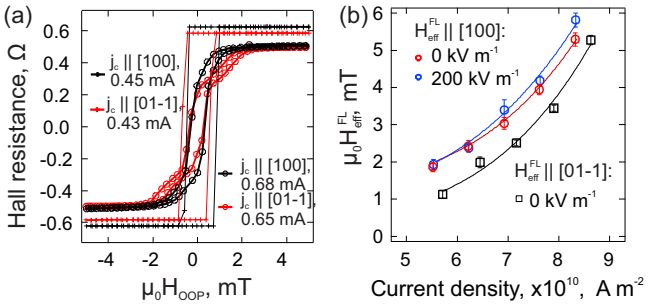

FIG. 3. (a) Anomalous Hall resistance during the OOP magnetic field sweep acquired for orthogonal directions of the current flow at room temperature and zero applied electric field across the PMN-PT substrate. The loops at higher currents have a significantly different shape indicating that the orthogonal directions are not equivalent even at zero field after electrical poling of the PMN-PT substrate due to hysteresis of the strain. (b) Comparison of the the field-like SOT effective field as a function of the current density measured along the orthogonal strain directions: $H_{\mathrm{eff}}^{\mathrm{FL}}$ along the compressive (red and blue) and $H_{\mathrm{eff}}^{\mathrm{FL}}$ along the tensile (black) strain directions at 0 kV m^{-1}. The field-like SOT effective fields measured in the direction of compressive strain are plotted for two magnitudes of the electric fields applied across the PMN-PT substrate. Note that the data points represent the average values of the two measured for opposite magnetization directions. The solid lines represent a power law fit to the data.

to the schematic in Fig. 1 (a) the FL SOT effective field is directed along the compressive strain direction. Note that the PMN-PT substrate was poled prior to any measurements, which resulted in the Hall cross device being no longer symmetric. This is reflected in the difference in the AHE hysteresis loop, shown in Fig. 3 (a), as well as in the measured FL SOTs for the orthogonal directions, in Fig. 3 (b). Furthermore, the electric field response of the FL SOT in this configuration has the opposite behavior. As seen in Fig. 3 (b), when the electric field is increased to 200 kV m^{-1}, the FL SOT effective field at high current densities becomes larger than that at zero electric field.

While the non-linear dependence of the FL torque on the current density measured at zero electric field can be attributed to the Joule heating effect and the M_{s} reduction at higher current densities, the change of FL SOT behavior with increasing electric field across the PMN-PT substrate needs to be explored. Since the strain does not significantly affect the M_{s} in our system, which is obtained from the strain dependence of the R_{AHE} (see Supplementary Materials), another mechanism has to be responsible for the observed behavior of the FL SOT. In order to understand the possible mechanism, we measured the variation of the PMA in our system at various currents and electric fields. The angle-dependent Hall voltage due to a DC current as a function of the constant external magnetic field of 200 mT was analyzed based on Stoner-Wohlfarth theory[29] for two strain directions. The magnitude of the DC current was chosen such as to provide similar shapes of the AHE hysteresis loop (and R_{AHE}) as in the harmonic Hall experiments. The estimated effective anisotropy field variation due to the tensile and compressive strain as a function of the DC current and for various electric fields are summarized in Fig. 4 (a) and (b), respectively. One can see, that $\mu_0 H_{\mathrm{eff}}$ decreases as a function of the applied DC current for all cases, which is consistent with the results of the harmonic Hall measurements discussed above.

One can also see that the increase of the electric field leads to the opposite response of the PMA in the case of tensile and compressive strain. As seen in Fig. 4 (a), $\mu_0 H_{\mathrm{eff}}$ measured using a DC current of 0.32 mA at zero electric field becomes smaller at 200 kV m^{-1}, i.e. when the magnitude of the tensile strain along the probing direction increases. On the contrary, the effective anisotropy field measured at 0.32 mA for the compressive strain increases with the increasing electric field magnitude (Fig. 4 (b)). This behavior is expected

since CoFeB is characterized by a positive magnetostriction coefficient,[30] i.e. under the in-plane tensile strain the magnetization in the CoFeB layer tends to incline towards the film plane, while compressive strain makes the out-of-plane direction more favorable for the magnetization.

Moreover, by comparing the current dependencies of the measured magnetic anisotropy for different magnitudes of the electric field across the PMN-PT substrate for single strain configuration, we can notice that the anisotropy change due to the increasing current is also different. As seen in Fig. 4 (a), $\mu_0 H_{\text{eff}}$ changes approximately by a factor of two when the DC current increases from 0.32 mA to 0.70 mA at zero field (red data set), while the measured change is less for 200 kV m^{-1}(blue data set). This can be understood assuming that the piezoelectric strain tends to counteract the anisotropy variation that results from the increasing current. On the contrary, the change of the anisotropy observed in Fig. 4 (b) becomes more pronounced for higher electric field magnitudes across the PMN-PT substrate, so that the strain in this case acts in the same way as the increasing current. This can be attributed to the strain-induced effects on thermoelectric properties of the system, e.g. opposite thermal conductivity variation due to tensile and compressive strain, which becomes increasingly relevant at the nanoscale.[31,32] As a result, application of strain of opposite sign leads to effectively different temperatures rise at the device due to the increased current,[33] which, in turn, reflects on the reduction of the magnetic anisotropy observed in Fig. 4. ~~This, however, is not intuitive, since naively thinking, it is the compressive strain, resulting in the PMA increase, this is expected to counteract the effect of heating, reducing the anisotropy.~~

We also find that the effect of strain on the magnetic anisotropy is smaller at higher DC currents for both strain directions. This can be attributed to the variation of the saturation magnetostriction, λ_s, which dictates the strength of the strain-induced magnetic anisotropy, $K_{\text{ME}} \propto \lambda_s Y \varepsilon$, where Y is the Young's modulus and ε is the generated strain.[10] Since the saturation magnetostriction for CoFeB itself was shown to follow M_s,[34] it can be expected that the strain effect on the magnetic anisotropy is less significant at higher currents, where also the M_s is reduced.

Thus, we can apply these findings to explain the current density dependencies of the FL SOT effective fields and their variation with the electric field applied across the PMN-PT substrate shown in Figs. 2 (c) and 3 (b). When the FL effective field is measured along the tensile strain direction (Fig. 2 (c)), where the piezoelectric strain impedes the anisotropy decrease at high currents (Fig. 4 (a)), the FL effective field slope reduces from the power law to approximately a linear dependence on the current. The opposite is observed for the compressive strain direction, acting together with the current-induced heating to decrease the anisotropy.

Therefore, by using electric field-induced strain it is possible to significantly tune the magnitude of the FL SOT effective fields, which according to the recent works can play a relevant role in magnetization dynamics in certain material stacks, where the FL torque can be much larger than its DL counterpart.[35–38] Furthermore, the HM/FM interface can also

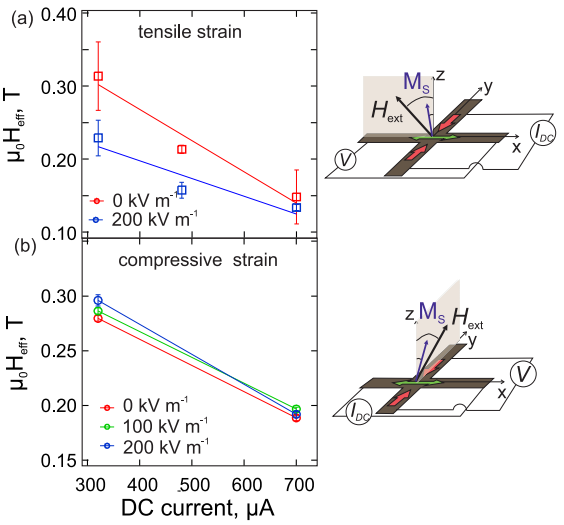

FIG. 4. PMA effective fields measured as function of the current for different electric fields across the PMN-PT substrate for (a) the tensile and (b) the compressive strain directions. The insets show the measurements geometries, where the angular dependence of the AHE was measured using an external magnetic field of $\mu_0 H_{\text{ext}} = 200$ mT directed along the tensile and compressive strain directions of the PMN-PT substrate.

give rise to a sizeable interfacial Dzyaloshinskii-Moriya interaction (DMI),[39,40] which originates from the inversion asymmetry with a strong SOC and can lead to the stabilization of topological spin textures,[41] such as homochiral domain walls and skyrmions.[42] Recent studies suggest that the joint action of the carefully tuned current-induced SOTs in such systems provides room for further optimization of the magnetization switching and even enables field-free switching[35,43] and ultrafast field-free deterministic creation of skyrmions on demand.[44] In this mechanism, the FL torque was found to either assist or impede the magnetization switching, depending on the relative strength of the FL torque.[35] Finally, the SOTs are also responsible for current-induced motion of skyrmions, which is fundamental for their potential use in efficient racetrack memories[45] or non-conventional computing.[18,46] Their immediate application, though, is hindered by the skyrmion Hall effect, i.e. that skyrmions move under an angle with respect to the driving current, which originates from the internal distortions of the non-trivial spin texture.[47,48] Recent work stresses the necessity to take into account the FL torques when considering the skyrmion dynamics,[48] as the anisotropy of these torques in HM/FM multilayer systems can introduce large corrections to the skyrmion Hall effect.[49,50] Thus, by tuning the asymmetry of the SOTs, which could be feasibly achieved with piezoelectric strain, one could control the skyrmion Hall effect and, as a consequence, the skyrmion motion, which is critical for their potential applications.

In conclusion, we show experimentally that the FL SOT in a Ta/CoFeB/Ta/MgO multilayer stack is significantly larger than the DL SOT and exhibits a non-linear dependence on the current density. This non-linear behavior can be explained

by a reduction of M_s as well as the perpendicular magnetic anisotropy due current induced heating, which is confirmed in the experiments. Moreover, we demonstrate that the magnitude of the FL SOT effective field can be efficiently manipulated by piezoelectric strain. We find consistent strain response of the FL SOTs with opposite dependence for strains of opposite signs. The FL SOT effective fields along the tensile strain direction, impeding the current-induced reduction of the PMA, can be drastically reduced by increasing the electric field applied across the piezoelectric substrate. On the contrary, larger electric fields lead to an increase of the FL SOT effective field along the compressive strain direction. This suggests that the FL SOTs in a Ta-CoFeB system can be modified differently by the piezoelectric strain, which could open a way to engineer and control the anisotropy of the SOTs in a system. The latter is potentially interesting as it can be used e.g. to tailor the skyrmion Hall angle, which is a necessary next step towards the use of skyrmions in device applications.

ACKNOWLEDGMENTS

We acknowledge that the work was financially supported by the Deutsche Forschungsgemeinschaft (DFG, German Research Foundation) in particular by Grant No. KL1811/18 (318612841) and the Graduate School of Excellence "Materials Science in Mainz" (DFG/GSC266) as well as European Union (ITN MagnEFi No.860060). L.B. acknowledges the European Union's Horizon 2020 research and innovation program under the Marie Skłodowska-Curie grant agreement ARTES number 793159.

DATA AVAILABILITY

The data that support the findings of this study are available from the corresponding author upon reasonable request.

[1] A. Manchon and S. Zhang, *Physical Review B* **78**, 212405 (2008).
[2] I. M. Miron, G. Gaudin, S. Auffret, B. Rodmacq, A. Schuhl, S. Pizzini, J. Vogel, and P. Gambardella, *Nature Materials* **9**, 230 (2010).
[3] J. Kim, J. Sinha, M. Hayashi, M. Yamanouchi, S. Fukami, T. Suzuki, S. Mitani, and H. Ohno, *Nature Materials* **12**, 240 (2013).
[4] K. Garello, I. M. Miron, C. O. Avci, F. Freimuth, Y. Mokrousov, S. Blügel, S. Auffret, O. Boulle, G. Gaudin, and P. Gambardella, *Nature Nanotechnology* **8**, 587 (2013).
[5] L. Liu, C.-F. Pai, Y. Li, H. W. Tseng, D. C. Ralph, and R. A. Buhrman, *Science* **336**, 555 (2012).
[6] A. Manchon, J.Železný, I. M. Miron, T. Jungwirth, J. Sinova, A. Thiaville, K. Garello, and P. Gambardella, *Rev. Mod. Phys.* **91**, 035004 (2019).
[7] T. Nan, J.-M. Hu, M. Dai, S. Emori, X. Wang, Z. Hu, A. Matyushov, L.-Q. Chen, and N. Sun, *Advanced Functional Materials* **29**, 1806371 (2019).
[8] M. Filianina, J.-P. Hanke, K. Lee, D.-S. Han, S. Jaiswal, A. Rajan, G. Jakob, Y. Mokrousov, and M. Kläui, *Physical Review Letters* **124**, 217701 (2020).
[9] H. Sohn, et al. *ACS Nano* **9**, 4814–4826 (2015).
[10] S. Finizio, et al. *Physical Review Applied* **1**, 021001 (2014).
[11] M. Filianina, et al. *Applied Physics Letters* **115**, 062404 (2019).
[12] M. Foerster, et al. *Nature Communication* **8**, 407 (2017).
[13] Y. Wang, L. Wang, J. Xia, Z. Lai, G. Tian, Z. Hou, X. Gao, W. Mi, C. Feng, M. Zeng, G. Zhou, G. Yu, G. Wu, Y. Zhou, W. Wang, X.-x Zhang, J. Liu, *Nature Communications* **11**, 3577 (2020).
[14] See `https://www.mtixtl.com`
[15] Q. Wang, et al. *Physical Review Applied* **10**, 034052 (2018).
[16] Huang, H. B., Zhao, C. P., & Ma, X. Q. *Advances in Condensed Matter Physics* **2016**, 9271407 (2016).
[17] G. Yu, P. Upadhyaya, X. Li, W. Li, S.K. Kim, Y. Fan, K.L. Wong, Y. Tserkovnyak, P.K. Amiri, K.L Wang, *Nano Letters* **16**, 1981 (2016).
[18] J. Zázvorka, F. Jakobs, D. Heinze, N. Keil, S. Kromin, S. Jaiswal, K. Litzius, G. Jakob, P. Virnau, D. Pinna, K. Everschor-Sitte, L. Rózsa, A. Donges, U. Nowak, M. Kläui, *Nature Nanotechnology* **14**, 658 (2019).
[19] T. Wu, P. Zhao, M. Bao, A. Bur, J. L. Hockel, K. Wong, K. P. Mohanchandra, C. S. Lynch, and G. P. Carman, *Journal of Applied Physics* **109**, 124101 (2011).
[20] S.B. Wu, T. Zhu, X. F. Yang, and S. Chen, *Journal of Applied Physics* **113**, 17C717 (2013).
[21] C. Zeng, Y. Yao, Q. Niu, H.H. Weitering, *Physical Review Letters* **96** 037204 (2006).
[22] R. Mathieu, A. Asamitsu, H. Yamada, K. Takahashi, M. Kawasaki, Z. Fang, N. Nagaosa, Y. Tokura, *Physical Review Letters* **93**, 016602 (2004).
[23] M. Hayashi, J. Kim, M. Yamanouchi, and H. Ohno, *Physical Review B* **89**, 144425 (2014).
[24] U. H. Pi, K. Won Kim, J. Y. Bae, S. C. Lee, Y. J. Cho, K. S. Kim, and S. Seo, *Applied Physics Letters* **97**, 162507 (2010).
[25] S. Emori, U. Bauer, S. Ahn, et al. *Nature Materials* **12**, 611 (2013).
[26] S. Yun, E. Park, K. Lee, S.H. Lim, *NPG Asia Mater* **9**, e449 (2017).
[27] X. Qiu, P. Deorani, K. Narayanapillai, K.-S. Lee, K.-J. Lee, H.-W. Lee, H. Yang, *Scientific Reports* **4**, 4491 (2014).
[28] D. Li, S. Chen, Y. Zuo, J. Yun, B. Cui, K. Wu, X. Guo, D. Yang, L. Wang, L Xi, *Scientific Reports* **8**, 12959 (2018).
[29] K.-W. Moon, J.-C. Lee, S.-B. Choe, K.-H. Shin *Review of Scientific Instruments* **80**, 113904 (2009).
[30] D. Wang, C. Nordman, Z. Qian, J. M. Daughton, J. Myers, *Journal of Applied Physics* **97**, 10C906 (2005).
[31] S. Bhowmick and V.B. Shenoy, *Journal of Chemical Physics* **125**, 164513 (2006).
[32] H.-F. Lee, S. Kumar, M.A. Haque, *Acta Materialia*, **58**, 6619 (2010).
[33] H. Fangohr, D.S. Chernyshenko, M. Franchin, T. Fischbacher and Guido Meier, *Physical Review B* **84**, 054437 (2011).
[34] L. Kraus, V. Haslar, P. Duhaj, *IEEE Transactions on Magnetics* **30**, 530 (1994).
[35] K. Wu, D. Su, R. Saha, J.-P. Wang, *Journal of Physics D: Applied Physics* **53**, 205002 (2020).
[36] C.O. Avci, K. Garello, C. Nistor, S. Godey, B. Ballesteros, A. Mugarza, A. Barla, M. Valvidares, E. Pellegrin, A. Ghosh, *Physical Review B* **89**, 214419 (2014).
[37] D. Wang, *Applied Physics Letters* **100**, 212405 (2012).
[38] J. Yoon, S.-W. Lee, J. H. Kwon, J. M. Lee, J.Son, X. Qiu, K.-J. Lee, H. Yang, *Science Advances* **3**, e1603099 (2017).
[39] T. Moriya, *Physical Review* **120**, 91 (1960).
[40] I. E. Dzyaloshinskii, *Journal of Physics and Chemistry of Solids* **4**, 241 (1958).
[41] A. Thiaville, S. Rohart, É. Jué, V. Cros, and A. Fert, *Europhysics Letters* **100**, 57002 (2012).
[42] A. Fert, N. Reyren, and V. Cros, *Nature Reviews Materials* **2**, 17031 (2017).
[43] B. Chen, J. Lourembam, S. Goolaup, S.T. Lim, *Applied Physics Letters* **114**, 022401 (2019).
[44] F. Büttner, I. Lemesh, M. Schneider, B. Pfau, C. M. Günther, P. Hessing, J. Geilhufe, L. Caretta, D. Engel, B. Krüger, J. Viefhaus, S. Eisebitt, G. S. D. Beach *Nature Nanotechnology* **12**, 1040 (2017).
[45] A. Fert, V. Cros, and J. Sampaio, *Nature Nanotechnology* **8**, 152 (2013).
[46] D. Prychynenko, M. Sitte, K. Litzius, B. Krüger, G. Bourianoff, M. Kläui, J. Sinova, K. Everschor-Sitte, *Physical Review Applied* **9**, 014034 (2018).
[47] W. Jiang, P. Upadhyaya, W. Zhang, G. Yu, M. B. Jungfleisch, F. Y. Fradin, J. E. Pearson, Y. Tserkovnyak, K. L. Wang, O. Heinonen, S. G. E. te Velthuis, and A. Hoffmann, *Science* **349**, 283 (2015).
[48] K. Litzius, I. Lemesh, B. Krüger, P. Bassirian, L. Caretta, K.Richter, F. Büttner, K. Sato, O. A. Tretiakov, J. Förster, R. M.Reeve, M. Weigand, I. Bykova, H. Stoll, G. Schütz, G. S. D.Beach, and M. Kläui, *Nature Physics* **13**, 170 (2017).
[49] J.-P. Hanke, F. Freimuth, B. Dupé, J. Sinova, M. Kläui, and Y. Mokrousov, *Physical Review B* **101**, 014428 (2020).
[50] K. Litzius, J. Leliaert, P. Bassirian, D. Rodrigues, S. Kromin, I. Lemesh, J. Zazvorka, K. Lee, J. Mulkers, N.Kerber, D. Heinze, N. Keil, R. M. Reeve,

M. Weigand, B. Van Waeyenberge, G. Schütz, K. Everschor-Sitte, G. S. D. Beach, M. Kläui *Nature Electronics* **3**, 30 (2020).

[51] A. Bisig, C. A. Akosa, J.-H. Moon, J. Rhensius, C. Moutafis, A. von Bieren, J. Heidler, G. Kiliani, M. Kammerer, M. Curcic, M. Weigand, T. Tyliszczak, B. Van Waeyenberge, H. Stoll, G. Schütz, K.-J. Lee, A. Manchon and M. Kläui, *Physical Review Letters* **117**, 277203 (2016).